

Shear Lag in Bolted Single Aluminum Angle Tension Members

C. Wang and C.C. Menzemer

(Submitted January 9, 2004)

Aluminum angles are widely used in engineering structures, examples of which include bracing in railcars, secondary members in ground transportation systems, scaffolding, and cooling towers. Often, aluminum angles are used as tension members with bolted end connections. Applicable design limit states include (a) yielding on the gross cross section, (b) tensile rupture through the net area, (c) progressive bearing failure, (d) bolt shear, and (e) block shear. As geometric considerations often preclude the connection of both legs of an angle, joint efficiency and tensile strength are reduced. The objectives of the experimental investigation include determination of the net section strength by physical tests of single aluminum angle tension members, examination of shear lag effects for several geometric parameters, and development of a more rational design approach.

Keywords aluminum, angles, bolted, shear lag, tension members

1. Introduction

Angles are used as tension members in many aluminum structural systems, examples of which include structural bracing in railcars, secondary members in ground transportation systems, construction and maintenance scaffolding, and cooling towers. Mechanically fastened joints are often used for aluminum tension members simply due to familiarity, past experience, and a relatively high degree of reliability. Proper design of bolted tension members requires due consideration of all appropriate limit states, including (a) yielding on the gross cross section, (b) net section tensile rupture, (c) progressive bearing distress, (d) fastener shear, and (e) tear-out of bolt groups (Ref 1, 2). Design provisions for bolted aluminum alloy tension members do not always provide adequate guidance for the estimation of net section tensile strength (Ref 3, 4). In particular, general procedures to account for the influence of unconnected cross-sectional elements on net section strength (sometimes referred to as shear lag) are lacking.

Geometric considerations often preclude the connection of both legs of an angle used as a tension member. As a portion of the angle is not available to transfer load, joint efficiency is reduced. A number of factors have been cited as having an influence on tension member joint efficiency, including material ductility, hole fabrication method, fastener spacing, connection length, and distance from the centroidal axis of the tension member to the plane of load transfer at the joint (Ref 5, 6). Shear lag is often cited as having a major influence on joint efficiency (Ref 7). Design provisions for structural steel tension members, as given by the American Institute for Steel

Construction (AISC), apply a shear lag reduction factor to the net area. The amount of the reduction is considered to be a function of load eccentricity and connection length and is given by:

$$U = 1 - \frac{x}{L} \quad (\text{Eq 1})$$

where U is the shear lag reduction coefficient, x is the distance from the centroid of the connected part to the plane of load transfer, and L is the connection length.

From the estimate of the shear lag reduction factor (U), it is a relatively simple matter to estimate the net section fracture strength of the angle as $P = (U A_n \sigma_u)$, where A_n is the net cross-sectional area of the angle and σ_u is the ultimate tensile strength of the material.

Current design provisions for bolted aluminum angle tension members are provided in the *Aluminum Design Manual* (Ref 8). For single aluminum angles used as tension members, the effective area of the net section is used as a means to estimate joint efficiency and net section strength. An effective section is estimated as the net area of the connected leg plus one-third of the area of the outstanding leg, irrespective of connection length, eccentricity in load transfer, ductility, fastener spacing, or fabrication method.

For this particular study, the primary goal was the development, or verification, of a general model to predict the net section strength of bolted, aluminum, single-angle tension members. To achieve this goal, physical tests were conducted. Experiments were used to determine the strength and behavior of the angles, as well as the strain distribution along critical cross sections. Information developed from the tests was used to examine models for the prediction of the net section tensile strength of the angles.

2. Material and Experimental Techniques

Materials chosen for this study included two aluminum-magnesium-silicon alloys (Aluminum Association designations 6061-T6 and 6063-T6). The as-received materials were pro-

C. Wang, DLZ Corporation, 6121 Huntley Rd., Columbus, OH 43229; and C.C. Menzemer, Department of Civil Engineering, The University of Akron, Akron, OH 44325-3905. Contact e-mail: ccmenze@uakron.edu.

vided in extruded lengths of different size angles. The nominal composition of each alloy is provided in Table 1. Table 2 summarizes the measured, typical, and guaranteed minimum tensile properties of each alloy. Materials used in this study were chosen to be common alloys so that extruded profiles of various sizes would be readily available. Further, the two alloys were chosen to provide a range of strengths typical of aluminum construction. Inspection of Table 2 reveals that the as-measured properties were similar and were closer to what would be considered typical for 6061-T6. As such, the results of the angle-strength tests were supplemented with limited data for angles of other alloys found in the literature (Ref 9, 10).

Samples for the angle-strength tests were prepared by sawing the extruded profiles to length in a horizontal band saw. Specimens were taken from angles with different cross-sectional dimensions, including $50 \times 50 \times 6.25$ mm ($2 \times 2 \times \frac{1}{4}$ in.), $64 \times 64 \times 6.25$ mm ($2.5 \times 2.5 \times \frac{1}{4}$ in.), $100 \times 100 \times 6.25$ mm ($4 \times 4 \times \frac{1}{4}$ in.), $100 \times 100 \times 9.5$ mm ($4 \times 4 \times \frac{3}{8}$ in.), and $150 \times 150 \times 12.5$ mm ($6 \times 6 \times \frac{1}{2}$ in.). All test samples used two, three, or four holes placed in a single line for the bolted connections (Fig. 1). Holes were marked on each sample in designated locations and were drilled 1.6 mm oversize to reflect actual tolerances. Nominal hole diameters varied from 19 to 25 mm. A total of 42 angles were fabricated. Table 3 summarizes the relevant geometric parameters of the specimens.

Figure 2 provides a schematic of the test setup. Gusset plates were attached to the testing machine through two-pin and clevis-type grips. Angles were bolted to each gusset plate. With the angles in place, some small amount of in-plane and out-of-plane rotation of the gussets was possible, providing for a degree of self-alignment. Each sample was mechanically tested in a universal testing machine (1330 kN or 300 kip load range). The machine has three calibrated scales, including a 53.4 kN (12 kip), a 267 kN (60 kip), and a 1330 kN (300 kip) load range. Smaller angles were tested using the 267 kN (60 kip) range, while the heavier-gage samples were evaluated using the 1330 kN (300 kip) load scale.

Data was recorded using a computerized data acquisition unit (Ref 11). Load and elongation were measured and recorded for each specimen tested. Load was read from a dynamometer attached to the testing machine. Elongation was mea-

sured by several linear variable displacement transducers (LVDTs). A single LVDT was mounted on the connected leg of the angle, while a second transducer was placed on the outstanding leg. Total elongation, including the elongation of the angle and the gusset plates, the deformation of the bolts, and the slip of the connection, was measured by the stroke of the testing machine. For a number of specimens, electrical resistance gages were used to record strain during the testing of the angles. Gages were typically mounted along the mid-length cross section of the samples as well as in the joint region. Strain gages were placed along a critical area, adjacent to the innermost bolts of the top or bottom connections (Fig. 3). All gages were oriented to measure strains in the longitudinal direction.

Samples were mounted to the gusset plates using bolts that were finger-tight. Approximately 10% of the expected yield load of the specimen was then applied to ensure that the bolts were bearing against the gusset plate and angle. While the load was applied, bolts were tightened to a “snug-fit” condition. After installation of the bolts, the load was released. An initial “zero” reading was then recorded, and testing commenced. At regular intervals, the displacement of the testing machine was held constant, and static load, elongation, and strain readings were obtained. Each sample was loaded in tension to failure.

In all cases, the angles failed through the net section as the ultimate load was obtained. Prior to tensile rupture, some necking was observed adjacent to the inward-most hole on one end of the angle. After necking, rupture occurred along the edge of the connected leg to the hole and proceeded to the corner of the angle (Fig. 4). Specimens would continue to carry load beyond the ultimate strength until the entire cross section was broken.

2.1 Experimental Results

Figure 5 shows a typical load-displacement plot for a $150 \times 150 \times 12.5$ mm ($6 \times 6 \times 0.5$ in.) angle. Sample SP5-3 used two bolts in the connection. As may be seen, the initial response is linear, up to a load of about 290 kN (80,000 lb). Beyond 290 kN (80,000 lb), the response is nonlinear, with deformation increasing at a faster rate than the corresponding increase in load. Final failure of the specimen occurred at a load of about 460 kN (121 kips). Table 4 summarizes the average failure load for each of the sample types tested. Average failure loads varied from about 111 kN (25 kips) for the $50 \times 50 \times 6.25$ mm ($2 \times 2 \times \frac{1}{4}$ in.) angles to a maximum of 579 kN (130 kips) for the $150 \times 150 \times 12.5$ mm ($6 \times 6 \times \frac{1}{2}$ in.) angles. In most instances, a minimum of three replicate samples was used to develop the average failure load. A total of 42 angles was tested and evaluated.

The experimental data were used to evaluate several different models for the calculation of the efficiency or shear lag

Table 1 Nominal composition of 6061 and 6063

Alloy	Composition, wt. %							bal
	Si	Fe	Cu	Mn	Mg	Cr	Zn	
6061	0.6	0.7	0.28	0.15	1.0	0.2	0.25	Al
6063	0.4	0.35	0.1	0.1	0.65	0.1	0.1	Al

Table 2 Tensile properties of 6061 and 6063 alloys

Alloy	Measured YS, MPa	Typical YS, MPa	Minimum YS, MPa	Measured UTS, MPa	Typical UTS, MPa	Minimum UTS, MPa
6061	280	255	241	301	290	262
6063	273	214	170	293	241	205

Note: YS, yield strength; UTS, ultimate tensile strength

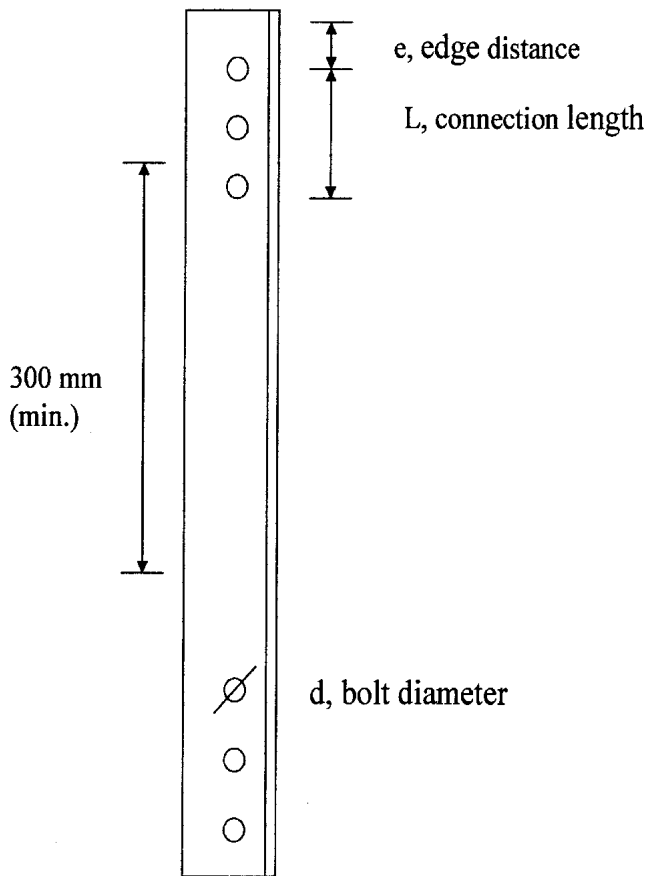


Fig. 1 Typical angle geometry

Table 3 Geometric parameters of the angles tested

Specimen	Size, mm	Hole diameter, mm	Number of bolts	Alloy	Connection length, mm
SP1-3	50 × 50 × 6.25	19	3	6063	114
SP1-4	50 × 50 × 6.25	19	4	6063	171
SP2-4	64 × 64 × 6.25	19	4	6061	229
SP2-3	64 × 64 × 6.25	19	3	6061	152
SP3-3	100 × 100 × 6.25	25.4	3	6063	203
SP3-4	100 × 100 × 6.25	25.4	4	6063	305
SP3-2	100 × 100 × 6.25	25.4	2	6063	102
SP4-3	100 × 100 × 9.5	25.4	3	6061	203
SP4-4	100 × 100 × 9.5	25.4	4	6061	305
SP4-2	100 × 100 × 9.5	25.4	2	6061	102
SP5-2	150 × 150 × 12.5	25.4	2	6061	57
SP5-3	150 × 150 × 12.5	25.4	3	6061	203
SP5-4	150 × 150 × 12.5	25.4	4	6061	305

factor. For each test result, an experimental shear lag factor was calculated from the maximum load obtained from individual tests as:

$$U = \frac{P_{\max}}{A_n \sigma_u} \quad (\text{Eq 2})$$

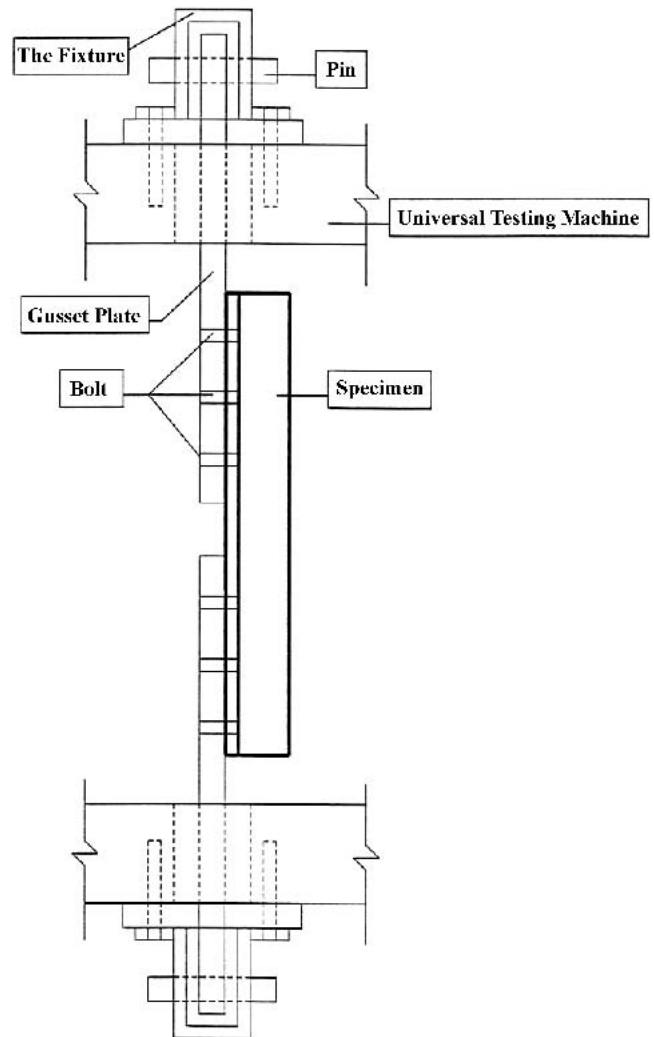


Fig. 2 Schematic of test setup

where P_{\max} is the maximum load obtained for the individual test sample, A_n is the net area of the sample, and σ_u is the measured ultimate tensile strength of the material.

Calculated values of the shear lag reduction factor were determined by examining several models that have been used for steel tension members, including the AISC approach as given by Eq 1. In addition, calculated values of the shear lag reduction factor were determined from a model originally developed by Kulak and Wu for steel angles (Ref 12). The shear lag reduction factor is determined by assuming that the net area of the connected leg of the angle is stressed to the ultimate tensile strength, and the gross area of the outstanding leg is stressed to some fraction of the yield strength. The maximum tension load supported by an angle may be given by:

$$P_{\max} = \sigma_u A_{cnl} + B \sigma_y A_{ol} \quad (\text{Eq 3})$$

where P_{\max} is the maximum tensile load the angle will support, σ_u is the ultimate tensile strength of the angle material, A_{cnl} is the net area of the connected leg, B is the fraction of the outstanding leg that is effective in the transfer of load, σ_y is the yield strength of the angle material, A_{ol} is the gross area of the

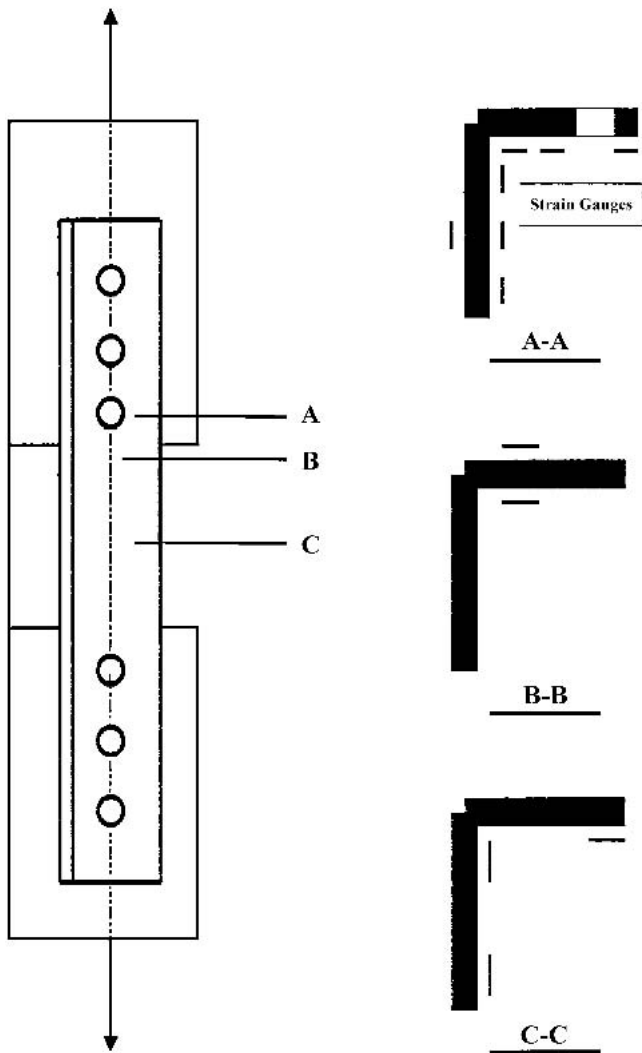


Fig. 3 Location of strain transducers on an angle

outstanding leg, and A_n is the net cross-sectional area of the angle.

By rearranging Eq 3, the shear lag reduction factor may be determined by:

$$U = \frac{1}{A_n} \left(A_{cnl} + B A_{ol} \frac{\sigma_y}{\sigma_u} \right) \quad (\text{Eq 4})$$

Figure 6 shows the variation of the average outstanding leg participation factor (B) with the number of bolts used in the connection. Indirectly, the number of bolts is indicative of the length of the connection. As may be seen, there is a significant difference between joints employing three or four bolts compared with angles connected by only two bolts. Two sets of B values were chosen for the range of behavior observed. For a lower bound, a participation value (B) of 0 was chosen for connections with two or fewer fasteners, while a value of 0.5 was taken for joints with three or more bolts. For an upper



Fig. 4 Failure of a 150 × 150 × 12.5 mm angle

Table 4 Average failure load for the angles tested

Specimen	Size, mm	Number of bolts	Average failure load, kN
SP1-3	50 × 50 × 6.25	3	111
SP1-4	50 × 50 × 6.25	4	113
SP2-4	64 × 64 × 6.25	4	128
SP2-3	64 × 64 × 6.25	3	121
SP3-3	100 × 100 × 6.25	3	225
SP3-4	100 × 100 × 6.25	4	229
SP4-3	100 × 100 × 9.5	3	324
SP4-4	100 × 100 × 9.5	4	344
SP4-2	100 × 100 × 9.5	2	294
SP5-2	150 × 150 × 12.5	2	419
SP5-3	150 × 150 × 12.5	3	550
SP5-4	150 × 150 × 12.5	4	579

bound, a B value of 0.33 was used for joints with two or fewer bolts, and a value of 0.66 was taken for connections with three or more fasteners.

Figure 7 compares shear lag reduction factors as given by Eq 1 and 4 with those calculated from the test results. As may be seen, shear lag reduction or joint efficiency, as determined by the application of Eq 1, provides values of U that are too large. As a result, the predicted values of the tensile rupture load would be expected to be unconservative. The application of Eq 4 with B values of 0 for joints with two bolts or less, and 0.5 for those with three or more, provide for better agreement between the test results and predicted values.

Professional factors were calculated for each individual angle tested. The professional factor is taken here to be the

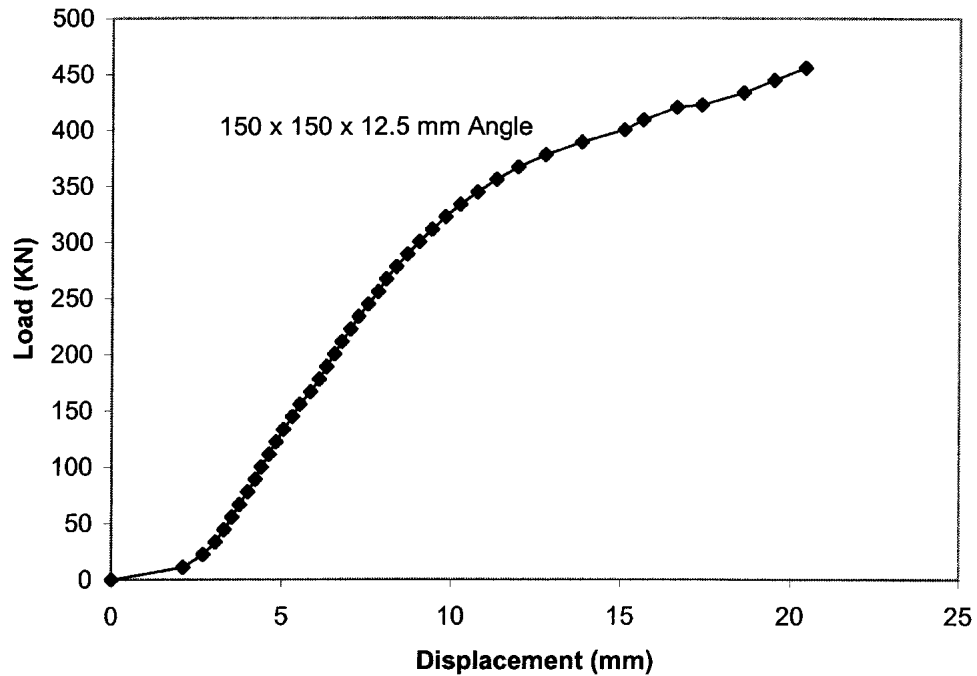


Fig. 5 Typical load displacement plot for a 150 × 150 × 12.5 mm angle

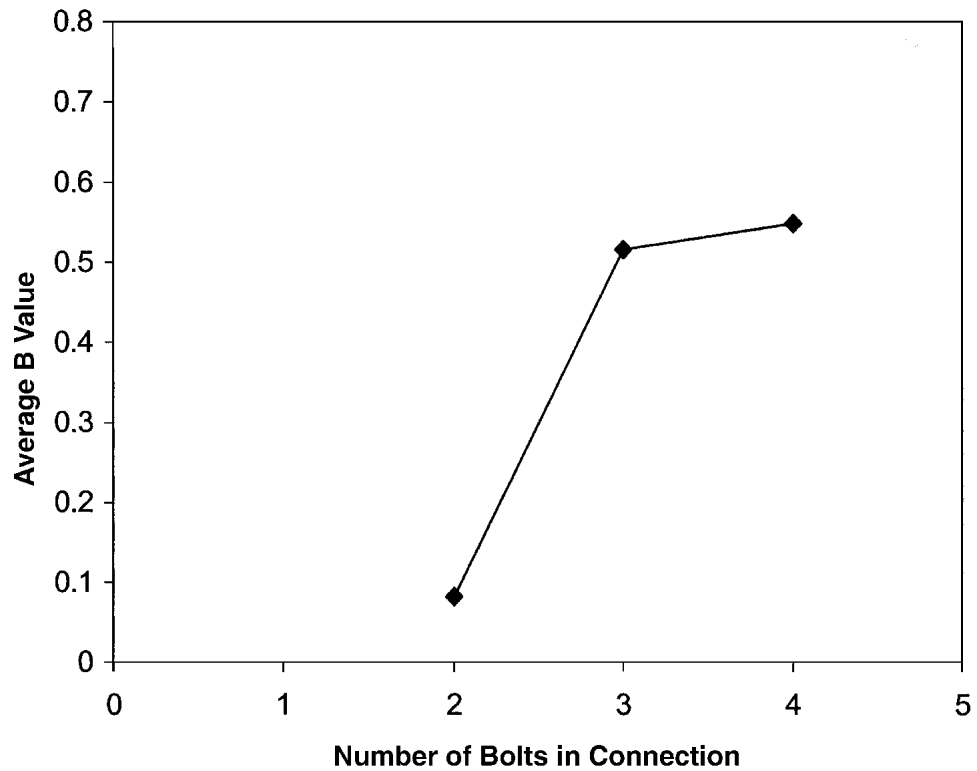


Fig. 6 Average value of *B* determined from test results

ratio of the predicted tensile rupture capacity of the angle to the actual test result. Figure 8 shows the professional factors for each angle, with the predictive models based on measured mechanical properties of the aluminum alloys used in the study.

Ideally, the ratio should be close to a value of 1.0, indicating agreement between the predicted capacity and the test result. For design purposes, a value of the professional factor close to, but slightly less than, 1.0 would be somewhat con-

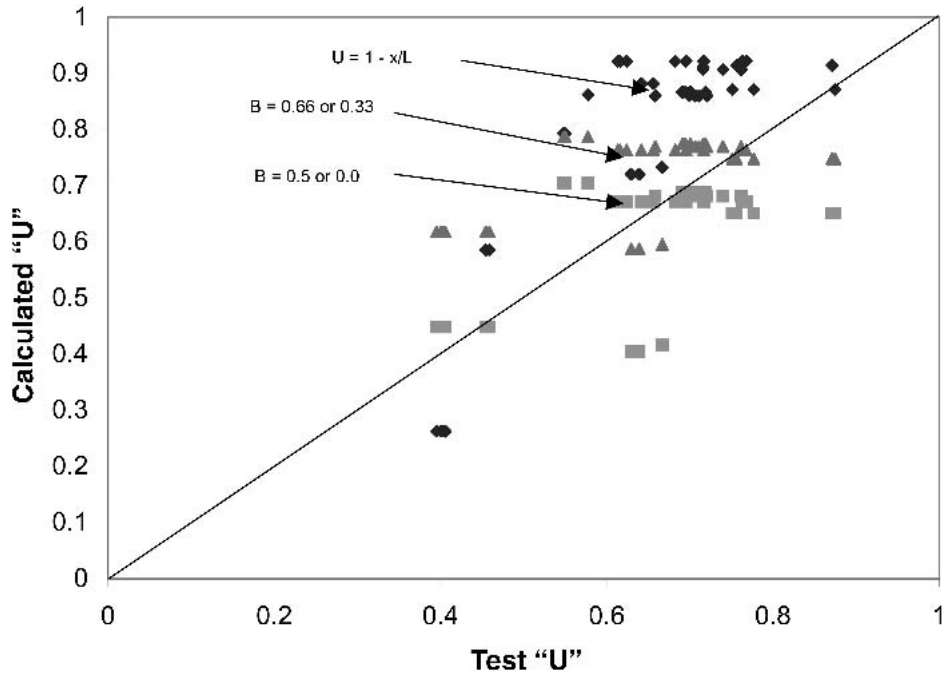


Fig. 7 Comparison of calculated shear lag reduction factors with values determined from the test results

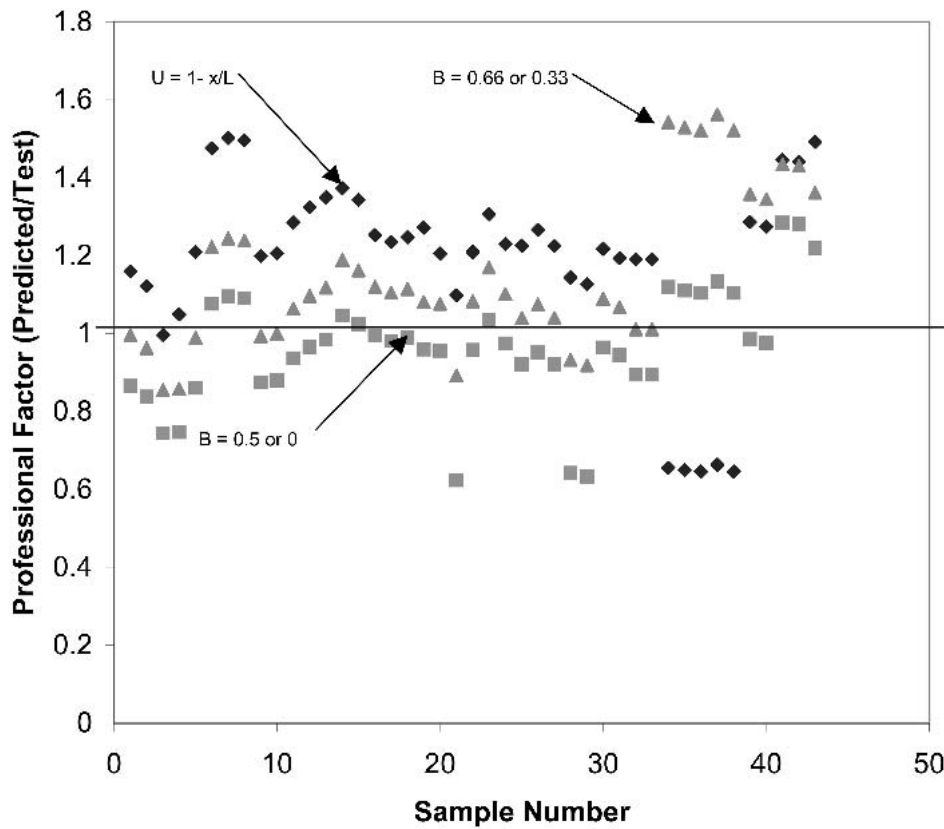


Fig. 8 Professional factors based on calculated strengths based on as-measured tensile properties and test results

servative. An examination of the data reveals that the application of Eq 3 with B values of 0 and 0.5 provides for a reasonable and, in most cases, a somewhat conservative estimate of

the fracture strength of the single-angle tension members. The use of Eq 1 to predict the tensile rupture strength provides unconservative results for a majority of the angles.

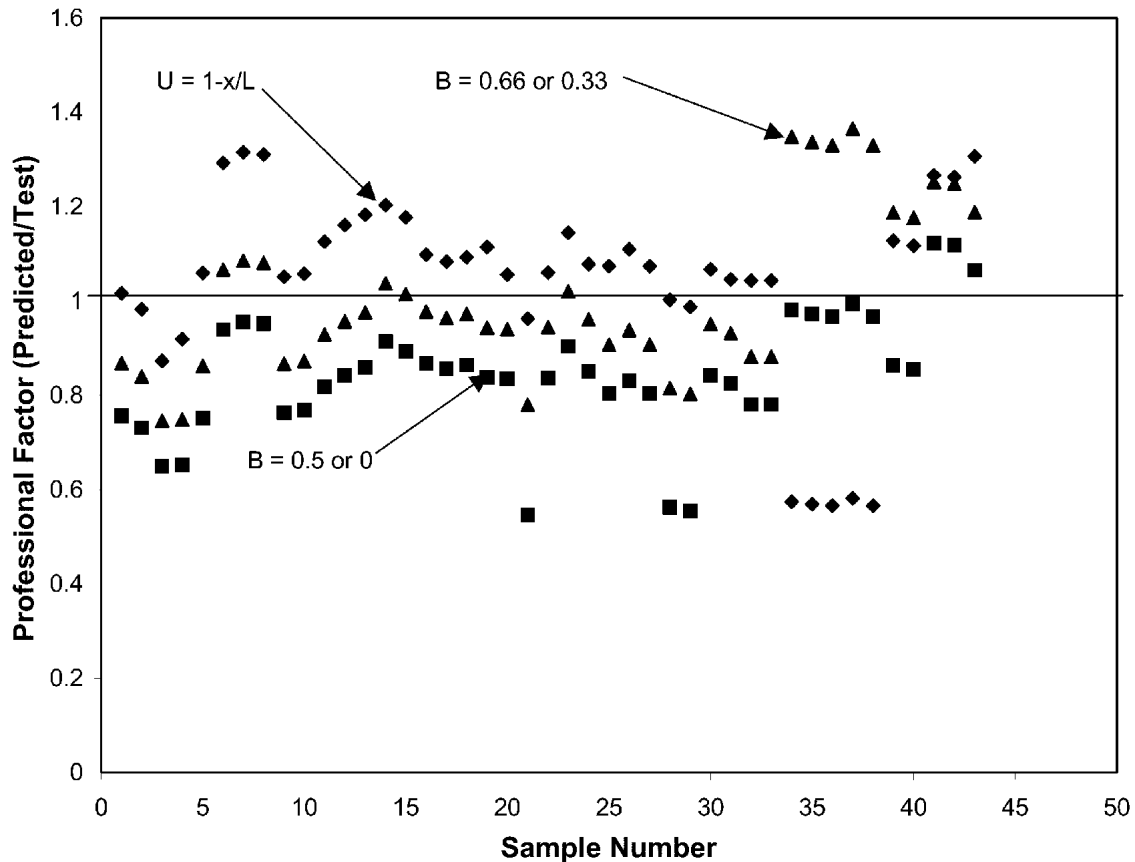


Fig. 9 Professional factors based on guaranteed minimum tensile properties

Figure 9 shows the professional factor for each angle. In this instance, the predicted values are based on the guaranteed minimum mechanical properties for the aluminum alloys used. The use of Eq 1 still, in a majority of cases, provides predictions of tensile rupture strength that are in excess of the test results. As such, the use of Eq 1 appears to be unsuitable for the estimation of the shear lag reduction factor used to estimate the net section tensile strength in the design of aluminum angle tension members attached by a single leg. As before, Eq 3 with values of B equal to 0 or 0.5 provides the most conservative estimates of tensile strength and is better suited for design purposes.

To further examine the use of Eq 3 to predict the fracture strength of aluminum angle tension members bolted through a single leg, data were obtained from the literature and were compared with the predictive model (Ref 9, 10). Figure 10 depicts the results of the comparison for a wide range of aluminum alloys. The solid lines represent the upper and lower bound strengths obtained from tests of the aluminum angles. In the case of aluminum alloys 2024 and 5456, only two data points were available, and the upper and lower bounds are almost identical. The results of the predictions are shown as individual data points. In general, the use of a participation factor of 0.5 for connections with three or more bolts, or 0 for two or fewer fasteners results in predicted fracture strengths that lie within the range of test results or are somewhat conservative. Only for aluminum alloys 2020 and 7178 does the

model using a participation factor (B) of 0.5 or 0 appear to be unconservative. In both cases, the range was established with just two data points, and may not represent the actual upper and lower bounds on strength. In the case of the aluminum alloy 2020, the model based on Eq 4 gave results that were nearly identical to the upper bound.

3. Conclusions

Based on the results of tests to determine the tensile rupture strength of aluminum angles connected by a single leg with bolts, the following may be ascertained:

- The traditional approach of evaluating the shear lag reduction factor by accounting for the eccentricity in load transfer and connection length (Eq 1) appears to be unconservative for aluminum angle tension members.
- A predictive model assumes the connected leg of the angle is stressed to the tensile ultimate, while the outstanding leg to some fraction of the material yield strength provides reasonable estimates of the net section fracture strength for a wide variety of aluminum alloys.
- The shear lag reduction factor may be given by:

$$U = \frac{1}{A_n} \left(A_{cnl} + B A_{ol} \frac{\sigma_y}{\sigma_u} \right)$$

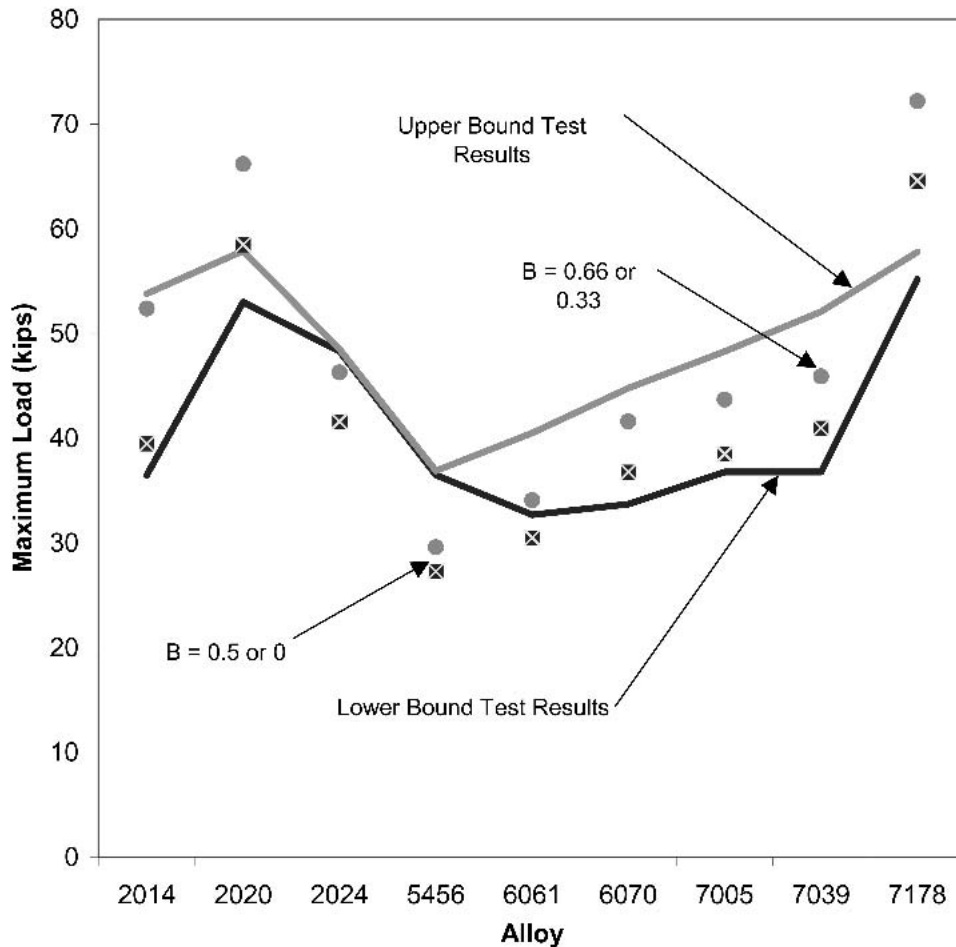


Fig. 10 Predictive model based on Eq 4 compared with the results of angle tests found in the literature

- A participation factor (B) may be taken to be 0.5 for connections with three or more bolts, and 0 for joints with less than two fasteners.
- The tensile strength of an aluminum angle attached by a single leg with bolts may be taken to be $P_{\max} = (U A_n \sigma_u)$.

Acknowledgments

This research was sponsored by The University of Akron (Akron, OH), RAVENS (Kent, OH), and the TGB Partnership (Hillsborough, NC).

References

1. R. Kissell and R. Ferry, *Aluminum Structures: A Guide to Their Specifications and Design*, John Wiley and Sons, 1995
2. Aluminum Company of America, *Alcoa Structural Handbook*, Aluminum Company of America, 1960
3. C. Menzemer, L. Fei, and T. Srivatsan, Design Criteria for Bolted Connection Elements in Aluminum Alloy 6061, *J. Mech. Design*, ASME, Vol 121, 1999, p 348-358
4. C. Menzemer, R. Ortiz, S. Shaffer, T. Srivatsan, and M. Petaroli, An Investigation of Confined Bearing Strength of AA5052 Aluminum Alloy, *Alum. Trans.*, Vol 2 (No. 2), 2000, p 337-343
5. W. Muse and E. Cheson, Riveted and Bolted Joints: Net Section Design, *J. Struct. Div.*, ASCE, Vol 89 (No. ST1), 1963, 107-126
6. S. Easterling and L. Giroux, Shear Lag Effects in Steel Tension Members, *Eng. J.*, AISC, Third Quarter, 1993, p 77-89
7. J. Fisher and J. Struik, *Guide to Design Criteria for Riveted and Bolted Joints*, John Wiley and Sons, 1974
8. The Aluminum Association, *Aluminum Design Manual*, The Aluminum Association, Washington, DC, 2000
9. M. Sharp, *Behavior and Design of Aluminum Structures*, McGraw-Hill, 1992
10. W. Dunn and R. Moore, "Tensile Tests of Aluminum Angles Loaded Through One Leg," Engineering Design Division Report 12-67-18, Alcoa, Sept 1967
11. Measurements Group, "System 5000: Model 5100 Scanner," Measurements Group, Raleigh, NC, 1995
12. G. Kulak and E. Wu, Shear Lag in Bolted Angle Tension Members, *J. Struct. Div.*, ASCE, Vol 123 (No. 9), 1997, p 1144-1152